

# Annual and seasonal variability in high latitude dust deposition, West Greenland

Maud A. J. van Soest<sup>1,2</sup>  | Joanna E. Bullard<sup>1</sup>  | Clay Prater<sup>1,3</sup>  |  
Matthew C. Baddock<sup>1</sup>  | N. John Anderson<sup>1</sup> 

<sup>1</sup>Geography and Environment, Loughborough University, Loughborough, Leicestershire, UK

<sup>2</sup>Centre for Ecology and Hydrology, Environment Centre Wales, Bangor, Gwynedd, UK

<sup>3</sup>Integrative Biology, Oklahoma State University, Stillwater, Oklahoma, USA

## Correspondence

Joanna E. Bullard, Geography and Environment, Loughborough University, Loughborough, Leicestershire LE11 3TU, UK.  
Email: [j.e.bullard@lboro.ac.uk](mailto:j.e.bullard@lboro.ac.uk)

## Abstract

High latitude regions ( $\geq 50^\circ\text{N}$  and  $\geq 40^\circ\text{S}$ ) are thought to contribute substantially to contemporary global dust emissions which can influence biogeochemical cycling as well as geomorphic, cryospheric and atmospheric processes. However, there are few measurements of the emission or deposition of dust derived from these areas that extend beyond a single event or season. This article reports the deposition of locally-derived dust to an ice-free area of West Greenland over 2 years from 23 traps distributed across five sampling sites. Local dust sources include glacial outwash plains, glacially-derived delta deposits and the reworking of loessic soils. Annual dust deposition is estimated at 37.3 to 93.9  $\text{g m}^{-2}$  for 2017–2018 and 9.74 to 28.4  $\text{g m}^{-2}$  in 2018–2019. This annual variation is driven by high deposition rates observed in spring 2017 of 0.48  $\text{g m}^{-2} \text{d}^{-1}$  compared to the range of 0.03 to 0.07  $\text{g m}^{-2} \text{d}^{-1}$  during the rest of the monitoring period. The high deposition rates in spring 2017 were due to warmer than average conditions and high meltwater sediment supply that delivered large quantities of sediment to local outwash plains in 2016. For other seasons, dust deposition was lower over both autumn–winter periods (0.03  $\text{g m}^{-2} \text{d}^{-1}$ ) than during the spring and summer (0.04–0.07  $\text{g m}^{-2} \text{d}^{-1}$ ). When sediment availability is limited, dust deposition increases with increasing temperature and wind speed. Secondary data from dust-related weather type/observation codes and visibility records were found to be inconsistent with measured dust deposition during the period of study. One possible reason for this is the complex nature of the terrain between the observation and sample sites. The dust deposition rates measured here and the infidelity of the observed dust with secondary data sources reveal the importance of direct quantification of dust processes to accurately constrain the dust cycle at high latitudes.

## KEYWORDS

aeolian, Arctic, dust codes, dust deposition, loess, proglacial, visibility

## 1 | INTRODUCTION

Glacial systems are very efficient at producing fine sediments in the form of silts. During past glacial periods the enhanced sediment supply from glacial processes contributed to atmospheric dust loadings that were substantially higher than at present (Albani et al., 2016; Mahowald et al., 2007). Under contemporary climatic conditions

glacier and ice-sheet extent has reduced and whilst glacial dust is still being generated it is largely confined to higher latitudes. High latitude dust has been defined as airborne particles  $< 100 \mu\text{m}$  in diameter originating from within the high latitudes ( $\geq 50^\circ\text{N}$  and  $\geq 40^\circ\text{S}$ ) and is thought to make a substantial contribution to the global annual dust budget (Bullard et al., 2016; Groot Zwaafink et al., 2016). Although dust originating from low latitudes is detectable in the Arctic

This is an open access article under the terms of the [Creative Commons Attribution](https://creativecommons.org/licenses/by/4.0/) License, which permits use, distribution and reproduction in any medium, provided the original work is properly cited.

© 2022 The Authors. *Earth Surface Processes and Landforms* published by John Wiley & Sons Ltd.

(vanCuren et al., 2012; Varga et al., 2021), it is increasingly recognized that dust sourced from high latitudes is important locally and regionally (Bullard, 2017). Both models and field data suggest that most northern hemisphere high latitude dust is retained within the Arctic region (Du et al., 2019; Groot Zwaafink et al., 2016) where it influences cryospheric, atmospheric, and marine and terrestrial ecological processes (Boy et al., 2019). For example dust derived from proglacial sources and deposited on the adjacent ice-masses can influence ice albedo and increase ice melt rates (Oerlemans et al., 2009). Dust can act as ice-nucleating particles in the atmosphere and affect cloud formation and hence radiative processes (Tegen, 2003; Tobo et al., 2019). Airborne dust transport can also provide a mechanism for transferring sediments and nutrients between disconnected parts of dry Arctic landscapes where hydrological connectivity is limited (Anderson et al., 2017), and dust deposition affects soil formation (Muhs, 2013; Muhs et al., 2004) and both terrestrial and marine nutrient availability (Arnalds et al., 2014; Crusius, 2021). Despite this, there remain very few contemporary studies that provide an understanding of the location and intensity of dust emissions, or the frequency, magnitude and timing of dust deposition that can be used to understand aeolian sediment fluxes at high latitudes (Beylich et al., 2016). This limits the extent to which high latitude dust, and its impacts on radiative and carbon budgets can be incorporated in to regional and global dust models (Cosentino et al., 2021; Crusius, 2021; Schmale et al., 2021).

The key drivers of dust emission from high latitudes are expected to be similar to those for low latitude dust emission and therefore to reflect the interaction of controlling variables within the aeolian sediment-system response framework (Bullard & McTainsh, 2003; Kocurek, 1998). These variables include sediment production (via weathering and erosion), transport capacity (wind speed and wind direction), sediment supply, sediment characteristics (such as size, sorting, shape) and modifiers of sediment availability such as crusting, vegetation and surface soil moisture (Bullard et al., 2016). Additional factors in cold regions can include frost, snow cover, temperature and humidity (Bullard, 2013). The input of high magnitude pulses of fine sediment to outwash plains due to catastrophic subglacial flooding may also be important in some locations (Prospero et al., 2012) but their significance is inconclusive (Bullard & Mockford, 2018; Nakashima & Dagsson-Waldhauserová, 2019). As at low latitudes, seasonal variation in dust emissions from high latitude sources is likely to reflect how the above variables combine to create suitable conditions for sediment entrainment and transport (Bullard et al., 2011; Zender & Kwon, 2005). For example, the timing of dust emissions from the Copper River valley in southern Alaska reflects the coincidence of elevated sediment availability, along-valley wind directions and minimal snow cover (Crusius et al., 2011). Regional variation in dust emissions across Iceland can be attributed to the role of snow cover preventing winter dust emissions from northern sources whilst dust emissions from largely snow-free southern sources occur year round with a spring peak associated with meltwater sediment supply (Bullard et al., 2016; Dagsson-Waldhauserová et al., 2013). Spatial patterns of deposition of locally-derived dust in the high latitudes are expected to reflect distance from source (e.g., reduction in quantity and grain size of deposits with increasing distance: Muhs et al., 2004) and the influence of topography on transport capacity (Goossens, 2006).

The aim of this study is to increase understanding of the spatio-temporal deposition of high latitude dust through field measurements in West Greenland. Two specific research questions were addressed. First, how much dust is deposited under contemporary conditions? This was determined using seasonal sampling, which also gives an indication of seasonal variability and of the environmental drivers associated with dust emission and deposition. Second, what are the sedimentological characteristics of the dust deposits and how do these vary temporally (seasonally) and spatially, with distance from the ice sheet? These observations will provide critical insights in to the interpretation of longer-term records such as loess deposits or lake sediment records as well as contributing to our understanding of the contribution of high latitude dust sources to the global dust budget.

## 2 | METHODS

### 2.1 | Study area and site selection

The occurrence of dust storms in Greenland has long been recognized (Fristrup, 1953; Hobbs, 1931) but most observations of modern dust events have been ad hoc (e.g., Dijkmans & Törnqvist, 1991) and research has been largely confined to long term or integrated records of deposition in soils, lake sediment cores and ice cores (e.g., Amino et al., 2021; Eisner et al., 1995; Willemse et al., 2003). Recent analyses suggest dust emission from ice-free areas of Greenland has increased over the past 20 years (Amino et al., 2021; Saros et al., 2019).

Our research is located around Kangerlussuaq (67°00'N, 50°43'20"W) in southwest Greenland, with the area of interest extending between the Greenland ice sheet (GrIS) margin and c. 40 km west of the ice sheet along a broad transect with an approximate latitude of 67°N (Figure 1). The mean annual temperature is  $-6^{\circ}\text{C}$ , characteristic of a continental arid interior with warm summers where temperatures can reach  $16^{\circ}\text{C}$  in early July (Anderson et al., 2012). Mean annual precipitation is  $< 200$  mm with most rainfall occurring in the late summer. The area has been extensively studied and is geomorphologically representative of many Arctic proglacial systems (Anderson et al., 2017). It includes floodplains with aeolian sand dunes, braided and meandering meltwater-fed river systems, raised marine terraces, moraine ridges, numerous lakes, low mountains and an extensive marine delta and fjord (Yde et al., 2018). Most locally-derived dust and region-wide loess originates from glacial floodplains which form from glacial weathering and riverine deposition of granodiorite (Eisner et al., 1995). Quartz, plagioclase, K-feldspar, amphibole, pyroxene and pyrite are the major minerals found in local glacial sediments (Hasholt et al., 2018).

Long-term aeolian activity in the region has been recorded in soils (Henkner et al., 2016; Ozols & Broll, 2003; Willemse et al., 2003) and lake sediments (e.g., Anderson et al., 2012; Rydberg et al., 2016; Saros et al., 2019). From these studies, modern aeolian deposition rates are estimated to be around  $70\text{ g m}^{-2}\text{ yr}^{-1}$ , and the sedimentary records indicate that whilst dust deposition has been continuous over the past 5000 years, it has been punctuated by more active periods and variations in particle size through time (Willemse et al., 2003).

There are few published measurements of contemporary dust deposition in the region. Engels (2003) collected dust from a lake

**FIGURE 1** Study area indicating location of study sites and Kangerlussuaq airport (marked with star on both inset and main maps) [Color figure can be viewed at [wileyonlinelibrary.com](https://onlinelibrary.wiley.com)]

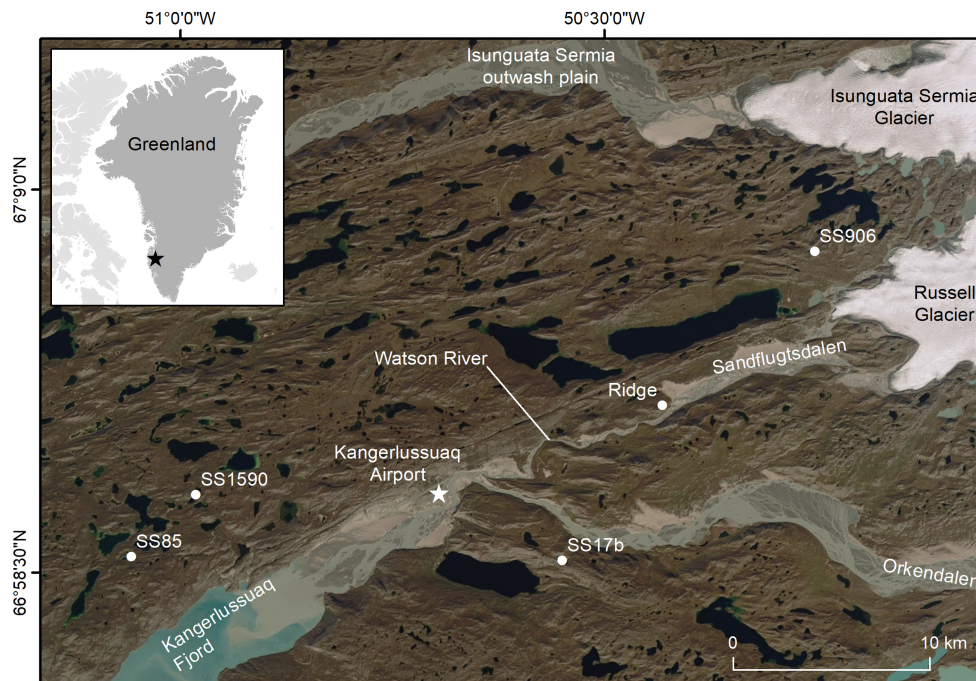


**TABLE 1** Summary of site characteristics

Name	Location (latitude/longitude)	Distance from GrIS margin (km)	Description
SS906	67°6'55.9044"N 50°15'58.1004"W	1.8	Lake catchment 400 m above sea level (a.s.l.). Low vegetation includes mosses, <i>Salix glauca</i> and <i>Betula nana</i> . Higher slopes are unvegetated or bedrock.
Ridge	67°3'36.0432"N 50°26'9.5208"W	5.6	Topographic ridge rising 75 m above Sandflugtsdalen outwash plain. North-facing slopes characterized by <i>B. nana</i> ; south-facing slopes feature grasses and <i>S. glauca</i> . Deflation patches are common.
SS17b	66°59'16.8216"N 50°33'0.3672"W	18.5	Lake catchment 235 m a.s.l. surrounded by steep (c. 25°) slopes. South-facing slope is rocky and unvegetated; north-facing slope features <i>B. nana</i> and <i>S. glauca</i> .
SS1590	67°0'52.5708"N 50°58'50.7396"W	33.4	East-west orientated lake catchment with two basins 200 m a.s.l. Surrounding slopes are steep with thin soils and sparse vegetation.
SS85	67°0'9.522"N 51°0'39.114"W	37.4	Lake catchment 190 m a.s.l. The south facing slopes are bare and sparsely covered with <i>S. glauca</i> . The north facing slopes feature <i>B. nana</i> .

catchment c. 20 km west of the ice-sheet margin over four consecutive 2 week periods in summer (2001) and calculated an average annual deposition rate of 2 to 8 g m<sup>-2</sup> yr<sup>-1</sup>. Fowler et al. (2018) sampled dust deposition over 14 days in July 2016 at a location c. 35 km west of the ice-sheet margin. The mean daily deposition rate was 0.931 g m<sup>-2</sup> d<sup>-1</sup>, which, if uniform through the year, would suggest an annual amount of 340 g m<sup>-2</sup> yr<sup>-1</sup>. These records only reflect relatively short sampling periods and were conducted mainly during the late spring or summer months. The occurrence and magnitude of any dust event captured during these short sampling periods will inevitably affect dust deposition estimates and is likely to result in an overestimate or underestimate of annual deposition rates. The contemporary seasonal pattern of dust emissions, based on a 70-year secondary dataset of World Meteorological Organization (WMO)

dust-related weather reporting codes, suggests a high frequency of dust events in spring and autumn driven by effective winds and sediment supply, and a decrease in frequency in summer months (July–August) (Bullard & Mockford, 2018).

To identify any patterns of dust deposition with distance away from the GrIS, this study focused on an east to west transect with five study sites between the ice sheet and the head of Kangerlussuaq fjord extending c. 40 km (Figure 1, Table 1). Four of the sites are small (< 10 km<sup>2</sup>), hydrologically-disconnected lake catchments. The fifth site is located on a ridge within the east–west oriented valley of Sandflugtsdalen which has previously been identified as one of the main regional dust sources (Eisner et al., 1995). The four lake catchment sites (prefixed SS) have previously been studied by other research groups (e.g., Anderson et al., 2001; Prater et al., 2021; Saros

et al., 2019) and the numerical labels used elsewhere have been retained here for consistency and to allow data relating to the catchments from this study to be associated with previous work.

## 2.2 | Dust sampling and analysis

Samples were collected using 24 cm diameter Hall Deposition Traps (HDT; Hall et al., 1993) which were deployed in April 2017 and sampled and re-set in June, August and April for two consecutive years (Table 2). Sampling seasons are hereafter referred to as spring (sediments collected in June), summer (sediments collected in August) and fall/winter (sediments collected in April). At each site, four or five traps were mounted on tripods with the trap head at a height between 1.5 and 1.8 m to minimize the capture of material transported by saltation. HDTs were located at different positions around each site to capture depositional variation related to local topography (Kidron et al., 2014). In some cases, when traps were visited to be emptied they had been knocked over or otherwise damaged by animals, consequently successful trap retrieval ranged from three to five per site. The sampling 'frisbee' part of each trap contains black foam (2.5 mm pore size) to trap deposited sediments and prevent re-entrainment by wind. The frisbee includes a central drain connected to a hollow tube which leads to a collection bottle. This prevents the frisbee filling with water and sediments being lost because the rainfall or snow melt drains in to the collection bottle taking any dust deposits with it. The 5-l collection bottles are black and contain 200 ml of 2-methoxyethanol biocide to reduce microbial growth. To retrieve sediments, the trap foam was removed and placed in the collection bottle, and any remaining material in the HDT head was washed into the collection bottle. Bottles and foams were then replaced with clean ones for the next sampling season and dust samples were stored frozen until further processing.

Particulate materials in dust collection bottles were vacuum filtered onto desiccated pre-weighed 0.45  $\mu\text{m}$  pore size nylon filters or 0.7  $\mu\text{m}$  glass fibre filters. Following desiccation, filtered samples were reweighed to obtain an estimate of dry mass deposition for each trap. After weighing, material was ashed at 500°C in a furnace for 4 h to remove all organic matter. The reciprocal of these loss-on-ignition (LOI) estimates was then multiplied by the dry mass value to obtain minerogenic dust masses for each trap and time period (i.e., the mass of inorganic material collected). Final areal dust deposition estimates (in  $\text{g m}^{-2} \text{d}^{-1}$ ) were calculated by accounting for trap diameter and collection period. Annual rates of dust deposition are estimated using a weighted average factoring in the number of days for each exposure. It should be noted that HDT trap efficiencies are unknown for cold climate conditions. Similar traps are estimated to be 20–40% efficient at wind speeds up to  $5 \text{ m s}^{-1}$  (Sow et al., 2006) but dust entrainment is not expected in this region until wind speeds exceed  $6 \text{ m s}^{-1}$  (Bullard & Austin, 2011; Dijkmans & Törnqvist, 1991). The expectation therefore is that our values of dust deposition are an underestimate. In addition, topography is known to result in different dust deposition rates on windward and leeward slopes (Comola et al., 2019; Goossens, 1996). Where the resultant direction of dust transport is consistent and unimodal this leads to distinctive spatial patterns of aeolian deposition (Muhs et al., 2004; Schaeztl et al., 2021); however, at the study sites used here sediment

TABLE 2 Dates of sampling periods and summary of key meteorological data

Season [abbreviation used in text]	Dates		Average wind speed ( $\text{m s}^{-1}$ )	Percentage time of wind speed > $6 \text{ m s}^{-1}$	Dominant direction for winds > $6 \text{ m s}^{-1}$	Total precip- itation (mm)	Temperature ( $^{\circ}\text{C}$ )		Visibility (km)	
	Start	End					Mean	Minimum	Mean	Minimum
Spring 2017 [Sp2017]	23 April 2017	20 June 2017	3.7	24	173	61	5.2	-14.6	41.2	0.6
Summer 2017 [Su2017]	21 June 2017	12 August 2017	4.2	26	143	103	10.7	-0.3	42.1	2.5
Autumn/winter 2017–2018 [FaW1718]	13 August 2017	13 April 2018	3.5	14	116	223	-10.1	-38.7	39.1	0.1
Spring 2018 [Sp2018]	14 April 2018	16 June 2018	3.7	31	191	26	0.6	-13.7	21.4	0.1
Summer 2018 [Su2018]	17 June 2018	13 August 2018	4.1	23	154	179	10.2	1.7	21.0	0.4
Autumn/winter 2018–2019 [FaW1819]	14 August 2018	13 April 2019	3.6	7	107	102	-9.3	-35.9	17.7	0.1

transporting winds are expected to be bimodal or multidirectional and to vary within and between seasons in response to local topographic and thermal drivers, and regional weather systems (Bullard & Austin, 2011; Bullard & Mockford, 2018; Heindel et al., 2015). The long trap exposure times used here mean that wind direction, and hence dust transport direction, is likely to be highly variable within each sampling period and the HDT trap most likely to capture highest rates of dust deposition will change from season to season. For this reason annual rates of deposition are calculated first using the median of all traps deployed during each season, and second using only the trap at each site that recorded the greatest total dust mass per sampling period.

Particle size analysis of the minerogenic material retrieved from the traps was conducted using a Beckman Coulter LS 230 laser sizer in the range 0.375–2000  $\mu\text{m}$  with 93 class intervals. Due to the low dust mass accumulated in some traps, at each site the sediment from

all the HDTs was bulked together to produce an average particle size distribution for each sampling period at each location.

### 2.3 | Environmental data

Meteorological data were used to determine the environmental conditions – wind speed, wind direction, precipitation, temperature – that occurred during the period of dust collection. Data were obtained from the WMO station at Kangerlussuaq airport (WMO 04231) located mid-way along the sampling transect (Figure 1). At the time of HDT sample collection, traps from the five different sites were retrieved over a period of several days as it was not logistically possible to empty and reset all the HDT traps in a single day. In order to associate the meteorological data with the dust data a representative single start and end date for each season was used (Table 2).

**TABLE 3** Minerogenic dust mass ( $\text{g m}^{-2} \text{d}^{-1}$ ) for each trap

	HDT	Sp2017	Su2017	FaWi1718	Sp2018	Su2018	FaWi1819
SS85	1	n/d	0.11	0.02	0.02	0.03	0.02
	2	n/d	0.11	0.03	0.07	0.18	0.02
	3	n/d	0.13	0.01	0.04	0.07	n/d
	4	n/d	0.06	0.02	0.05	0.04	n/d
	5	n/d	0.07	n/d	n/d	0.09	0.01
	Mean		0.09	0.02	0.04	0.08	0.02
	Median		0.11	0.02	0.05	0.07	0.02
SS1590	1	0.72	0.05	n/d	n/d	0.02	0.05
	2	0.39	0.06	n/d	n/d	0.02	0.03
	3	0.48	0.06	0.01	0.01	0.05	0.04
	4	0.08	0.05	0.02	0.02	0.02	0.04
	5	0.56	0.06	n/d	0.09	0.05	0.02
	Mean	0.44	0.06	0.01	0.04	0.03	0.04
	Median	0.48	0.06	0.02	0.02	0.02	0.04
SS17b	1	0.39	0.12	0.03	0.04	0.09	0.02
	2	0.10	0.06	0.03	0.04	0.08	n/d
	3	0.25	0.04	0.02	0.03	0.04	n/d
	4	0.15	0.03	n/d	0.06	0.04	0.02
	5	0.53	0.03	n/d	n/d	0.04	0.03
	Mean	0.28	0.06	0.03	0.04	0.06	0.02
	Median	0.25	0.04	0.03	0.04	0.04	0.02
Ridge	1	0.74	0.05	0.05	0.06	0.03	0.02
	2	0.98	0.09	0.02	0.04	0.04	0.02
	3	0.11	0.04	0.02	0.04	0.03	0.02
	4	0.66	0.08	0.02	0.04	0.02	0.01
	Mean	0.62	0.06	0.03	0.05	0.03	0.02
	Median	0.7	0.07	0.02	0.04	0.03	0.02
SS906	1	0.42	0.03	0.11	0.03	0.02	0.03
	2	0.78	0.04	0.03	0.03	0.06	0.02
	3	0.83	0.09	0.01	0.03	0.05	n/d
	4	n/d	0.05	n/d	n/d	n/d	0.03
	Mean	0.68	0.05	0.05	0.03	0.04	0.02
	Median	0.78	0.05	0.03	0.03	0.05	0.03

Note: n/d denotes trap not deployed or damaged during deployment.

The measurements of dust deposition are cumulative for each season and it is not possible from these to determine the extent to which deposition resulted from a single or few large dust events, or multiple small events. Secondary data, such as WMO dust codes (Dagsson-Waldhauserova et al., 2014; O'Loingsigh et al., 2014) and visibility records (Mahowald et al., 2007; Xi, 2021), are widely used for long-term studies and broadscale mapping of dust activity and their use is explored here to determine whether they can provide some insight into the magnitude and frequency of dust events contributing to overall deposition at the seasonal scale. The WMO defines 11 different internationally-recognized weather codes relating to dust events and the dust codes recorded at Kangerlussuaq airport were extracted from the meteorological record. Strong relationships have been found between visibility and atmospheric dust concentration both close to source and regionally (10–100 km from source; Baddock et al., 2014; Leys et al., 2011; Wang et al., 2008). Leys et al. (2011) associate visibility of  $\leq 0.2$  km with a severe dust storm,  $> 0.2$ – $1.0$  km with a moderate dust storm,  $> 1.0$ – $5.0$  km with a severe dust haze and  $> 5.0$ – $10.0$  km with a moderate dust haze. Visibility is recorded hourly at the airport meteorological station and was also used to determine the potential frequency of different types of dust event as defined by visibility.

In addition to aeolian transport capacity, a key control on dust emissions is sediment supply which in proglacial areas can be closely linked to meltwater suspended sediment transport (Bullard, 2013). The main dust sources in the Kangerlussuaq region are proglacial outwash plains and delta sediments at the head of Kangerlussuaq fjord which are regularly replenished by the deposition of meltwater suspended sediments from the Watson River (Hasholt et al., 2013). Previous research has identified a positive relationship between the concentration of suspended sediments predominantly  $\leq 2$  mm diameter and discharge from the Watson River (Hasholt et al., 2018). We therefore used published meltwater discharge data for the Watson River (van As et al., 2019) as an indication of potential sediment supply to the floodplain dust sources. An additional dust source may be from the reworking of loess deposits which extend from the ice sheet margin to approximately 70 km west (Heindel et al., 2015).

## 3 | RESULTS

### 3.1 | Dust deposition measurements

Minerogenic dust deposition was recorded at all sites and for all sampling periods. Daily rates of dust deposition across the whole data collection period ranged from  $0.01 \text{ g m}^{-2} \text{ d}^{-1}$  to  $0.98 \text{ g m}^{-2} \text{ d}^{-1}$  for individual traps and the mean dust deposition per site (all seasons) ranged from  $0.06 \text{ g m}^{-2} \text{ d}^{-1}$  to  $0.14 \text{ g m}^{-2} \text{ d}^{-1}$  (Table 3). Figure 2 shows the variability in daily dust deposition for each site by season. Spring 2017 recorded the highest rates of dust deposition with median values ranging from  $0.25$  to  $0.7 \text{ g m}^{-2} \text{ d}^{-1}$  per site and an overall median deposition for all traps of  $0.48 \text{ g m}^{-2} \text{ d}^{-1}$ . The next highest seasonal median value is summer 2017 ( $0.06 \text{ g m}^{-2} \text{ d}^{-1}$ ). The fall/winter deposition rates are the same for both years at  $0.02 \text{ g m}^{-2} \text{ d}^{-1}$ . Spring and summer 2018 have the same median deposition rates of  $0.04 \text{ g m}^{-2} \text{ d}^{-1}$ . The annual dust deposition estimated using a weighted average (median) to account for the different trap exposure periods, and using all traps, is  $37.3 \text{ g m}^{-2}$  for 2017–2018 and

$9.74 \text{ g m}^{-2}$  for 2018–2019. The annual deposition estimated using only the trap recording the highest dust mass per site is  $93.9 \text{ g m}^{-2}$  for 2017–2018 and  $28.4 \text{ g m}^{-2}$  for 2018–2019.

Figure 3(a) summarizes the cumulative dust deposition measured at the four sites where samplers were deployed for the full 2 year period. This excludes data from SS85 where sampling did not start until summer 2017. The highest median cumulative dust deposition was recorded at the two sites closest to the GrIS, SS906  $62.29 \text{ g m}^{-2}$  (1.8 km) and the Ridge  $61.58 \text{ g m}^{-2}$  (5.6 km). Less dust was deposited overall at SS17b, 18.5 km from the ice ( $25.99 \text{ g m}^{-2}$ ). At SS1590, 33.4 km from the ice, the median cumulative dust deposition was  $47.2 \text{ g m}^{-2}$ . Excluding the data from spring 2017 enables change over a longer distance to be examined by including data from SS85 and removes the unusually high values from this season (Figure 3b). For this record, median values for all sites are similar and in the range  $12.61$ – $17.78 \text{ g m}^{-2}$ . Quantities of dust in each trap are highly variable when spring 2017 is included in the data but variability is considerably reduced at all sites when it is removed (Figure 3). Without the exceptionally high values from spring 2017, there is no systematic regional change in the quantity of dust deposition with distance from the GrIS.

### 3.2 | Dust particle-size characteristics

The mean particle size of material for all sampling periods was in the range  $7$ – $36 \mu\text{m}$  indicating trapped sediments predominantly comprise fine to coarse silts (Figure 4). At all sites, the particle size distribution is fine-skewed and multimodal with one or more dominant silt modes ( $< 63 \mu\text{m}$ ) and a minor secondary clay mode ( $< 2 \mu\text{m}$ ). The proportion of particles  $< 2 \mu\text{m}$  ranges from 3.1% to 14.2% for all sites and seasons. In all seasons except summer 2018, the dominant mode at each site is in the medium, or fine-medium silt range. The dust deposits captured in summer 2018 have a higher proportion of coarser particles ( $> 32 \mu\text{m}$ ) with the dominant mode ranging from  $41 \mu\text{m}$  (Ridge) to  $111 \mu\text{m}$  (SS1590; coarse silt to very fine sand). During both summer sampling periods the sediments trapped at SS906 (1.8 km from the GrIS) are coarser than at other sites. Figure 5 summarizes the change in sediment texture of the dust deposits with distance from the ice sheet and by season. There is very little change in the proportion of particles  $< 2 \mu\text{m}$  trapped with distance from the ice sheet which is typically c. 10% in spring and fall/winter but less than 10% in summer.

### 3.3 | Secondary dust data

During the entire period of trap deployment the WMO station at Kangerlussuaq airport recorded five out of the 11 possible WMO dust codes on 13 different days (Table 4). In 2017–2018 dust codes were only recorded on 2 days, both in June 2017, and were codes 6 and 7 (dust haze and raised dust, respectively). In 2018–2019 dust codes were recorded on 11 days distributed across all seasons and of these one was a moderate event (code 31), and six were severe events (code 34). In most cases dust was only recorded for 1 to 2 h, the exception being the event of 16 August 2018 which was observed over 6 h. Wind speed observed at the same time as the dust events varied from  $1$  to  $21 \text{ m s}^{-1}$  and wind direction was typically from the

**FIGURE 2** Seasonal variation in dust deposition per site by season and year. Box plots indicate median (bold line), first and third quartiles. Note: y-axis scale differs for each plot

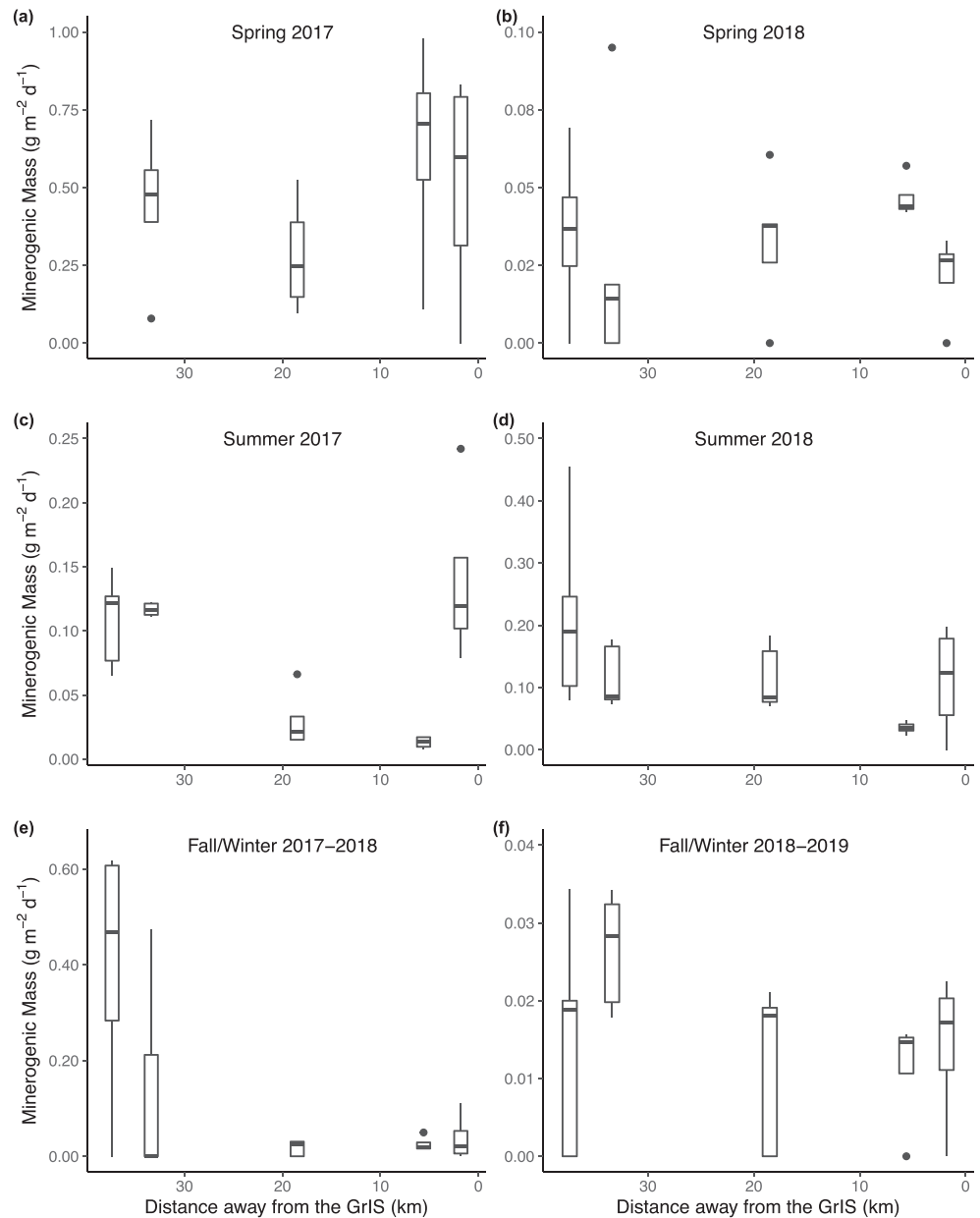
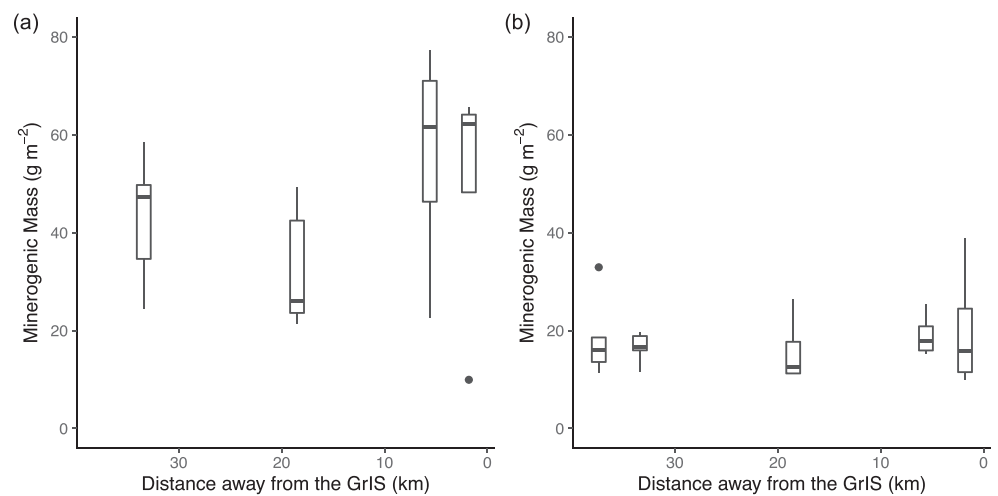


**FIGURE 3** (a) Total dust deposition (entire sampling period) by site with distance away from the GrIS. Panel excludes SS85 (37.4 km) for which no spring 2017 data are available. (b) Dust deposition from summer 2017 to fall/winter 2018–2019, that is excluding spring 2017. Box plots indicate median (bold line), first and third quartiles



northeast–east–northeast (down valley) or southwest–west (up-valley). The average visibility from the airport was  $\geq 37$  km (Table 2); however, on every day of the sampling period visibility was

reduced to  $\leq 10$  km for at least one observation per day (Table 5). Visibility was reduced to  $\leq 0.4$  km on each occasion that a code 34 event was noted but for all other dust codes visibility was  $>$

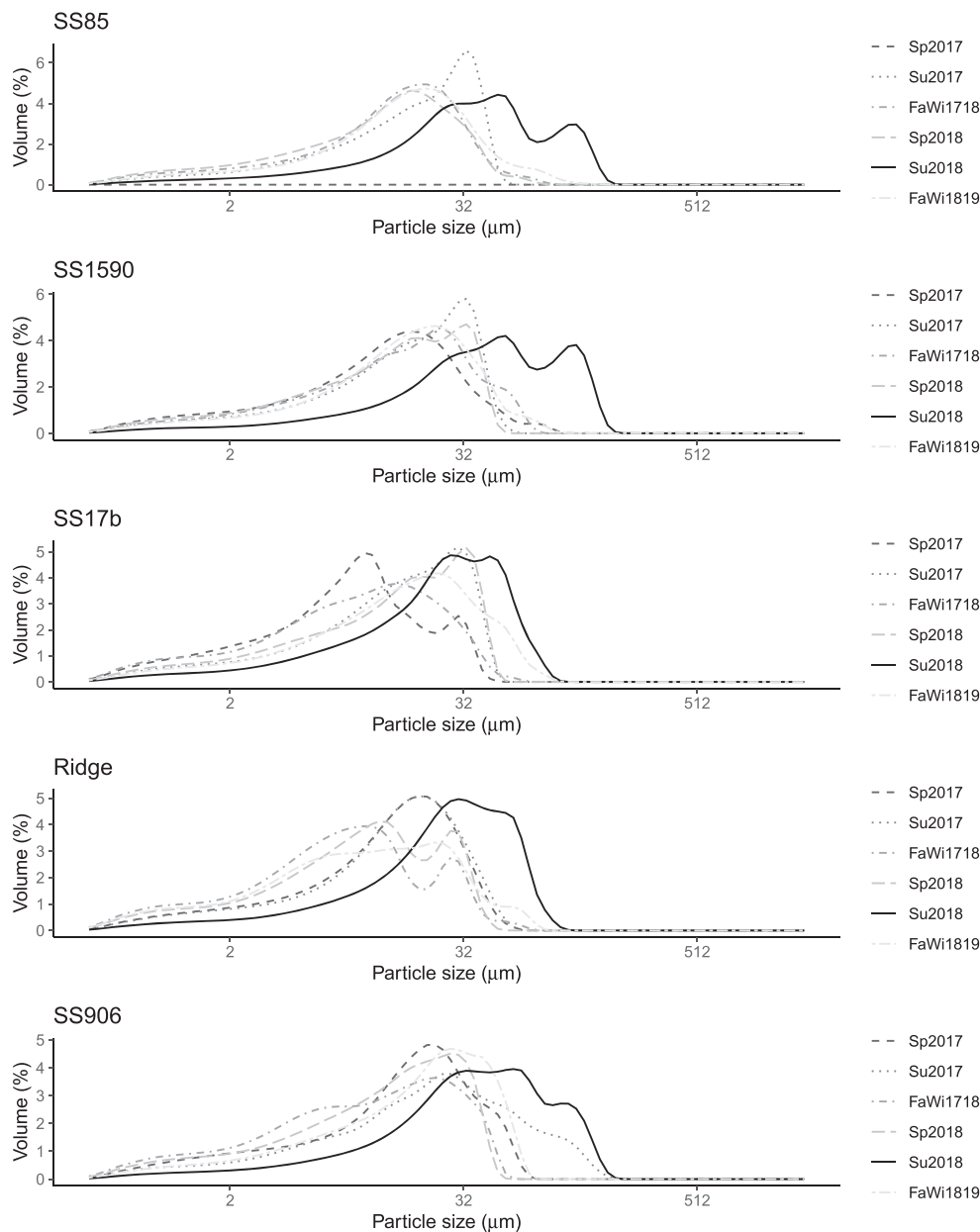


**FIGURE 4** Particle size distribution by season of dust deposits averaged for all traps at each site

1 km (Table 4). Table 5 summarizes the frequency of days with at least one observation at which visibility was reduced to  $\leq 10$  km, which includes 16 days where visibility  $\leq 0.2$  km. Visibility reduction was recorded most frequently during the fall/winter in both years.

### 3.4 | Environmental drivers

Meteorological data for the sampling periods are summarized in Table 2. The mean wind speed was highest for both summer seasons ( $> 4 \text{ m s}^{-1}$ ) and in the range  $3.5\text{--}3.7 \text{ m s}^{-1}$  for all other sampling periods. Field observations by Dijkmans and Törnqvist (1991) and Bullard and Austin (2011) suggest a typical wind speed threshold of  $6$  to  $7 \text{ m s}^{-1}$  is required to entrain silts and fine-medium sands in the region. Allowing for the different lengths of the sampling periods, the seasons with the highest frequency of winds  $> 6 \text{ m s}^{-1}$  are spring and summer (averaging  $> 5 \text{ h d}^{-1}$ ) whilst the fall/winter periods have the lowest frequency. Windspeeds stronger than  $10 \text{ m s}^{-1}$  were recorded mostly in the two winter seasons and spring 2018. For all seasons, the

dominant direction for winds  $> 6 \text{ m s}^{-1}$  is southerly in the spring and broadly south-easterly in the other sampling seasons. Total precipitation includes both rain and snow and was higher in the summer and in line with long-term patterns.

The long-term baseline (1981–2010) temperatures at Kangerlussuaq are  $-7.2^\circ\text{C}$  (March–April–May),  $+9.5^\circ\text{C}$  (June–July–August),  $-4.4^\circ\text{C}$  (September–October–November) and  $-18.7^\circ\text{C}$  (December–January–February). For logistical reasons, the sampling periods used here overlap the traditional definition of ‘seasons’ or are partial. For example FaWi1718 includes late summer (end August), all of autumn (September, October, November), winter (December, January, February) and early spring (March to mid-April). Spring 2018 in turn runs from mid-April to mid-June, that is excludes early spring and includes early summer. Nevertheless, the average temperature for each ‘season’ as defined here corresponds to the long-term temperature pattern but with spring and fall/winter means being higher than the standard baseline at least partly due to their incorporation of part of the summer or spring period, respectively (Table 2). In spring 2016, the year preceding deployment of the dust traps, a new high spring

**FIGURE 5** Summary of particle size characteristics with distance away from the GrIS grouped by season

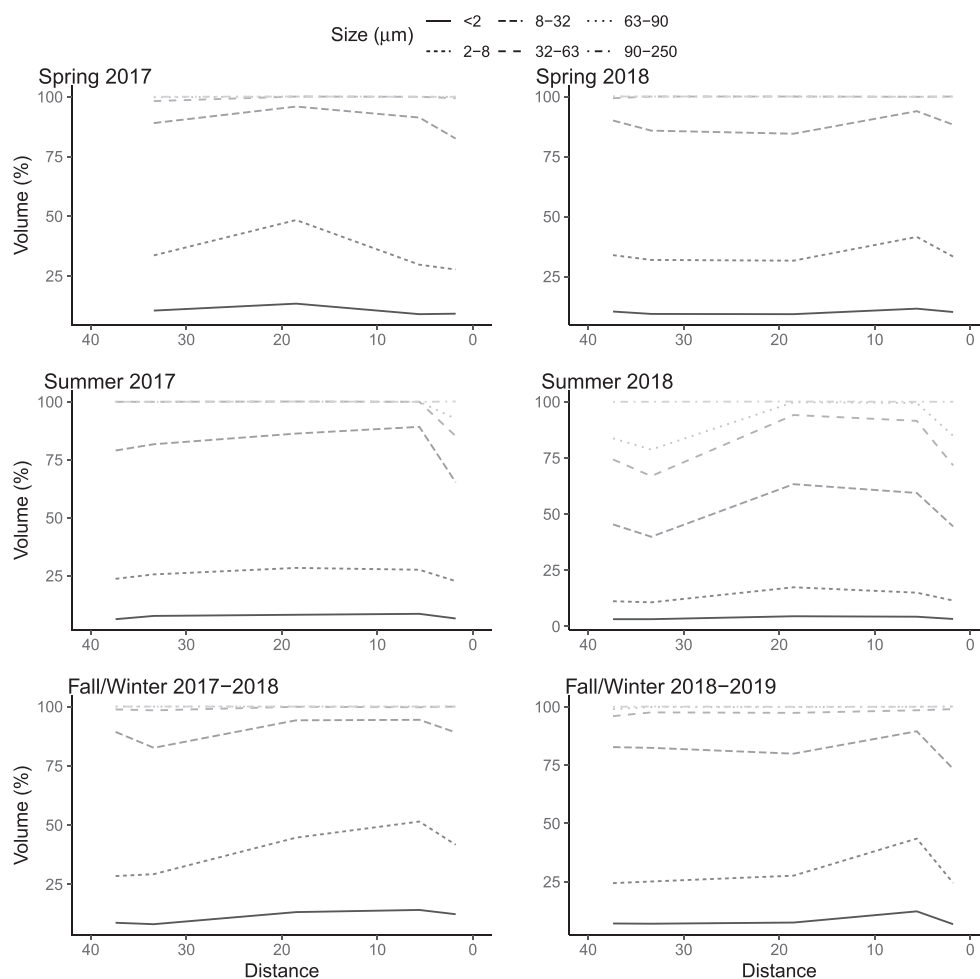


**TABLE 4** World Meteorological Organization (WMO) weather codes related to dust (from O’Loingsigh et al., 2014) and associated wind speed, direction and visibility records recorded at Kangerlussuaq between April 2017–April 2019. Where multiple visibility records are available for a single event only the lowest is reported here

SYNOP code	Weather description	Date reported	Duration (h)	Wind speed (m s <sup>-1</sup> )	Wind direction (deg)	Visibility (km)
6	Widespread dust in suspension in the air, not raised by wind at or near the station at the time of observation.	5 June 2017	1	21	250	5.6
7	Dust or sand raised by wind at or near the station at the time of observation, but no well-developed dust whirl(s) or sand whirl(s) and no dust storm or sandstorm seen.	16 June 2017	1	18	250	2.2
		17 May 2018	1	24	100	6.2
		28 June 2018	1	16	n/a	6.2
		27 October 2018	1	13	60	3.1
9	Dust storm or sand storm within sight at the time of observation, or at the station during the preceding hour.	3 October 2018	1	18	250	4.4
31	Stable slight or moderate sand or dust storm with visibility < 1000 m but > 200 m.	9 March 2018	1	6	60	6.2
34	Stable severe dust storm with visibility < 200 m.	19 March 2018	1	2	50	0.2
		22 April 2018	2	1–2	60–260	0.1
		18 July 2018	2	1–3	110–130	0.2
		16 August 2018	6	1–7	50–240	0.1
		13 December 2018	1	6	50	0.4
22/ December 2018	1	6	60	0.2		

**TABLE 5** Average total dust deposition measured per sampling period and frequency of days with reduced visibility

Season	Total dust deposition (g m <sup>-2</sup> )	Number of days with visibility reduction			
		≤0.2 km	0.2–1 km	>1–5 km	>5–10 km
Sp2017	28.4	0	3	13	59
Su2017	3.5	0	0	10	53
FaWi1718	6.9	7	32	114	244
Sp2018	2.6	3	6	27	65
Su2018	2.9	1	1	9	58
FaWi1819	6.1	5	32	91	243

temperature record was set with a temperature anomaly of 6.7°C. Seasonal temperature anomalies during the field sampling period were typically < 1°C with the exception of spring 2019 where temperatures were 2.5°C above the baseline (Tedesco et al., 2018).

The relationship between dust deposition recorded during each sampling period and the average air temperature, wind speed and precipitation during the same period is shown in Figure 6. For the measurements recorded here, spring 2017 is a clear outlier with dust deposition an order of magnitude higher than the other sampling periods and for all sampling periods there is no relationship between dust deposition and meteorological conditions. Excluding data from spring 2017, there is a positive significant relationship between seasonal dust deposition and both mean air temperature and wind speed.

Mean annual discharge from the Watson River from 2006 to 2018 was 6.47 km<sup>3</sup>. In 2016, the year prior to this study, discharge was very high, at 8.2 km<sup>3</sup> ± 1.3 km<sup>3</sup> triggered by the record high spring temperatures. In 2017 and 2018 discharge was below average at 4.3 ± 0.6 km<sup>3</sup> and 3.76 ± 0.66 km<sup>3</sup>, respectively (van As et al., 2019).

## 4 | DISCUSSION

### 4.1 | Seasonal and annual dust deposition rates and drivers

Rates of dust deposition measured over short time periods are highly variable and inevitably depend on whether or not the measuring period coincides with dust emission events. The individual daily trap rates of dust deposition for this study (0.01–0.98 g m<sup>-2</sup> d<sup>-1</sup>) are comparable with previous short-term measurements in the Kangerlussuaq area by Fowler et al. (2018; 0.93 g m<sup>-2</sup> d<sup>-1</sup>) and our site averages (0.06–0.16 g m<sup>-2</sup> d<sup>-1</sup>) are similar to those from high latitude locations in southern South America (0.014–0.158 g m<sup>-2</sup> d<sup>-1</sup>; Cosentino et al., 2021). Previous studies have suggested year-round dust emissions in Kangerlussuaq with peaks in spring and autumn (Bullard & Mockford, 2018) but also with dust storms in the winter (Hobbs, 1931). Engels (2003) reported dust accumulation values over a snow season (October 2000–April 2001) of 1.97 to 4.33 g m<sup>-2</sup> which suggests a daily rate of 0.01–0.02 g m<sup>-2</sup> and corresponds well to the 0.03 g m<sup>-2</sup> d<sup>-1</sup> winter rates reported here.

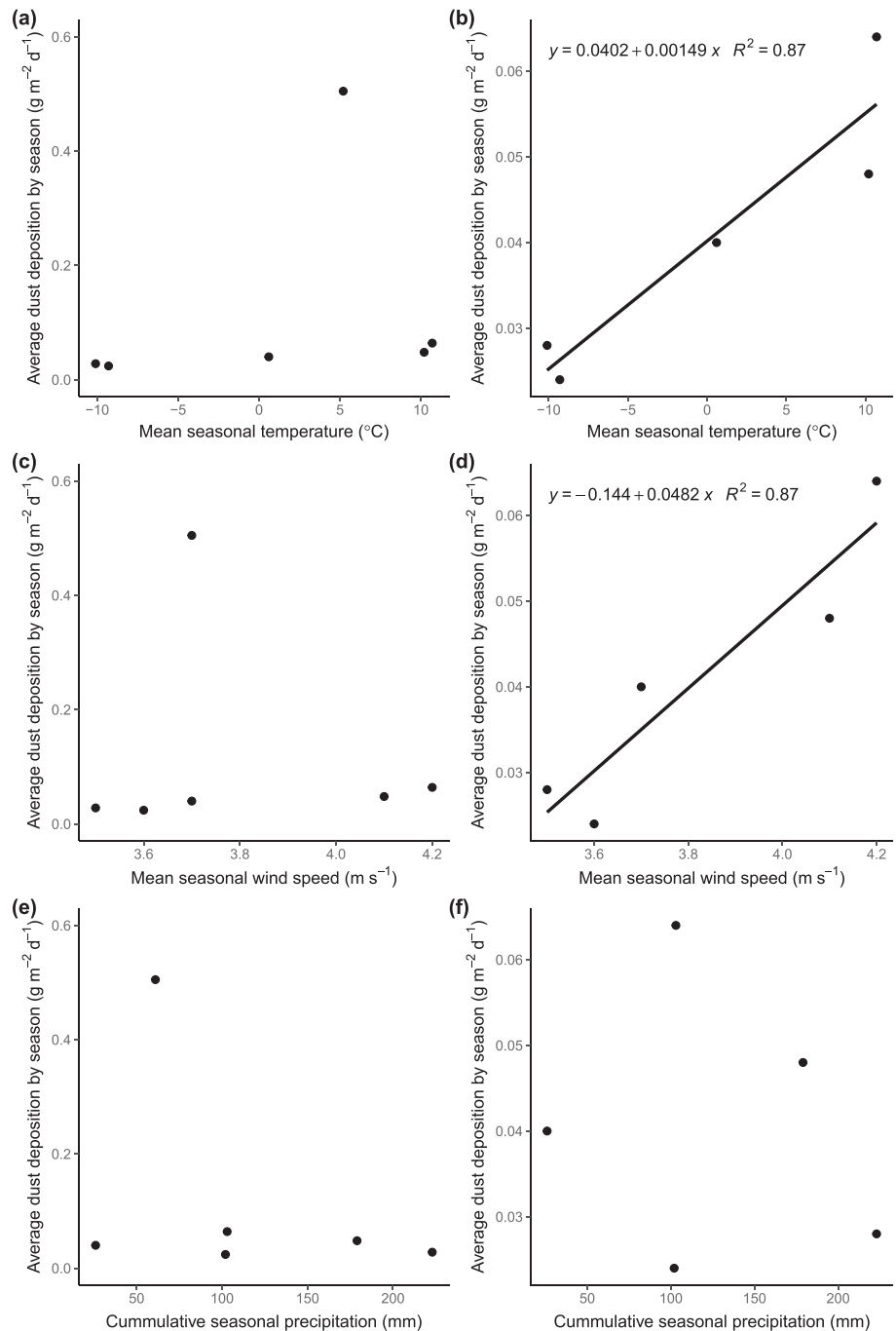
Annual estimates of dust deposition rates vary considerably from location to location and with distance from their dust source(s). Lawrence and Neff (2009) conducted a meta-analysis of global dust deposition rates in > 50 areas and found typical deposition rates of

50 to 500 g m<sup>-2</sup> yr<sup>-1</sup> occurring within 10 km of the dust source, 1–50 g m<sup>-2</sup> yr<sup>-1</sup> within 10–1000 km of the source ('regional' deposition) and ≤ 1 g m<sup>-2</sup> yr<sup>-1</sup> at more than 1000 km from source. In the Kangerlussuaq region, there are multiple dust sources (Figure 1) and bidirectional winds which mean that all the traps deployed for this study are within 20 km of one of the active outwash plains or fjord delta. The estimates of annual dust deposition reported here are 9.74–37.3 g m<sup>-2</sup> yr<sup>-1</sup> (trap average per site) or 28.4–93.9 g m<sup>-2</sup> yr<sup>-1</sup> (highest deposition rate per site) and are consistent with the local to regional values suggested by Lawrence and Neff (2009). They are also the same order of magnitude as those reported from high latitude regions of New Zealand (26.4 g m<sup>-2</sup> yr<sup>-1</sup>; Marx & McGowan, 2005), southern South America (40 g m<sup>-2</sup> yr<sup>-1</sup>; Cosentino et al., 2020), British Columbia (11 g m<sup>-2</sup> yr<sup>-1</sup>; Owens & Slaymaker, 1997) and low-medium deposition areas in Iceland (13–117 g m<sup>-2</sup> yr<sup>-1</sup>; Arnalds, 2010).

Previous estimates of annual dust deposition around Kangerlussuaq range from 2 g m<sup>-2</sup> (extrapolated from short-term summer sampling; Engels, 2003) to 70 g m<sup>-2</sup> (Willemse et al., 2003). The 2 years of dust deposition in West Greenland reported here suggest considerable interannual variability. This is to be expected as most studies from dust emission regions in both low and high latitudes report highly variable seasonal and annual deposition rates. This variability is typically driven by the seasonal interplay of factors affecting sediment supply, availability and transport capacity (Bullard, 2013; Zender & Kwon, 2005) interacting with large scale periodic climate patterns such as El Niño-Southern Oscillation (Cosentino et al., 2020; Li et al., 2021; Marx et al., 2009). With only a 2-year record of measurements it is not possible to examine the impact of climate periodicity on West Greenland dust emissions, but there are sufficient data to consider seasonal drivers.

From the overall quantity and particle-size characteristics of the dust sampled during this study, we can infer that the dust is entrained from proximal sources (< 100 km) within Greenland, rather than having been transported long distances (Lawrence & Neff, 2009; Tsoar & Pye, 1987). Further support for this comes from the multi-modal particle-size characteristics of the dust deposits which closely correspond to those of the suspended load (Lund-Hansen et al., 2010) and outwash plain deposits (Bullard & Austin, 2011) of the Watson River. Many studies of dust deposition are carried out in locations a considerable distance from the contributing dust source; however, in this case both emissions (not reported here) and deposition are associated with environmental conditions local to the study sites. The amount of dust in the

**FIGURE 6** The relationship between total dust deposition and average temperature, wind speed and precipitation. Panels on the left including data for spring 2017. Panels on the right exclude data for spring 2017



atmosphere reflects how much sediment is available for entrainment and the transport capacity of the wind which meteorologically are linked directly or indirectly to wind speed, temperature and precipitation. Typically, where sediment is available, an increase in wind speed leads to an increase in the amount of dust in the atmosphere and an associated increase in dust deposition (Figgis et al., 2018; Lancaster, 2002; Offer & Goossens, 2004; O'Hara et al., 2006; Reheis & Urban, 2011). For the results reported here, there is a significant positive relationship between wind speed and dust deposition if the data from spring 2017 are excluded. In spring 2017, dust deposition was an order of magnitude higher than in all the other sampling periods, but wind speeds were not notably high. This suggests sediment supply and availability may have been more important controls on dust deposition in spring 2017 than transport capacity.

The main sediment supply for dust emissions around Kangerlussuaq is from suspended sediments in meltwater following their deposition across the outwash plains and delta area (Bullard & Austin, 2011; Dijkmans & Törnqvist, 1991). A time lag can occur between the deposition of meltwater sediments and wind entrainment that produces dust emissions which can vary from hours to months and may be caused by sediments being wet, frozen or snow-covered, or low wind speeds (e.g., Dagsson-Waldhauserova et al., 2013; Mockford et al., 2018; Prospero et al., 2012). Discharge from the Watson River in 2016 – the year before this study – was  $8.2 \pm 1.3 \text{ km}^3$ , one of the highest since 2006 (van As et al., 2019). Hasholt et al. (2018) identified a positive relationship between suspended sediment concentration and discharge for the Watson River from which we can infer that meltwater sediment supply was high that year and this may have resulted in a greater supply of fine

sediments to the Sandflugtsdalen outwash plain and/or reworking of the floodplain resulting in a fining upwards sequence of sediments suitable for wind erosion (Bullard & Austin, 2011).

Once supplied to the outwash plain, these sediments may not immediately be available for entrainment due to high moisture content and/or below threshold winds. Sediment availability may also be limited by low temperatures causing freezing of sediments or snow cover during the winter. With a time lag between meltwater deposition of sediments on the outwash plain, sufficient desiccation for erodibility and the occurrence of above threshold winds, this priming input of sediment supply in summer 2016 may account for the very high rates of dust deposition recorded during spring 2017. Subsequent annual discharge of the Watson River was below average (4.3 km<sup>3</sup> in 2017; 3.76 km<sup>3</sup> in 2018) which is less likely to have replenished the outwash plains possibly explaining the comparatively low dust deposition rates measured in subsequent seasons.

With regards to other meteorological variables, some studies have found a positive relationship between concurrent dust deposition and temperature (e.g., O'Hara et al., 2006; Rymer et al., 2022) attributed to higher temperatures causing drying of the sediment surface and lowering the threshold for wind entrainment but this is not universal. As with wind speed, there is a significant relationship between dust deposition and temperature for the Kangerlussuaq region for sampling periods excluding spring 2017 (Figure 6). Finally, in this study, there is no relationship between dust deposition and precipitation. There are few reports of any relationship between dust deposition and precipitation for concurrent intervals but several studies have found a relationship between antecedent precipitation and high dust emissions (McTainsh et al., 1998; Offer & Goossens, 2004; Reheis & Urban, 2011). In warmer regions, the time lag between precipitation and dust deposition has been linked to a temporary reduction in sediment availability for example due to ephemeral vegetation suppressing dust emissions (Mao et al., 2013; McTainsh et al., 1998) or the formation of dust-inhibiting physical and/or biological surface crusts in response to rainfall (Bullard et al., 2022). Established biological crusts are present at the Kangerlussuaq study sites and form on, and protect, wind-eroded soils (Heindel et al., 2019) but factors directly affecting sediment availability on the outwash plains such as moisture availability (Mockford et al., 2018) or the development of a protective lag deposit (Bullard & Austin, 2011) are likely to have a greater influence on overall dust emissions.

The earlier-mentioned suggests that when sediment availability is limited, dust deposition reflects contemporary meteorological conditions. When sediment availability is unlimited, the amount of dust available for deposition is increased but, as observed in other studies, there could be a time lag between increased sediment supply and dust emissions.

## 4.2 | Relationship between measured dust deposition and secondary records

A wide range of studies has used dust-related weather codes to map spatio-temporal patterns of dust activity but there have been few attempts to compare field quantification of dust processes with these proxy data. In the Kangerlussuaq area, some observations of suspended dust plumes have coincided with dust codes recorded at

the WMO station. Dijkmans and Törnqvist (1991) describe an event that coincided with a code 7 record (September 1987) and Engels (2003) noted a 'very large' event on 23 June 2001 which was logged at the WMO station (1400 h, code 7; 1800 h, code 8) but also an 11.5 h event on 20 June which was not coincident with a dust code record. Our data suggest inconsistencies between the measured deposition data and what the dust codes indicate in the Kangerlussuaq area. Bullard and Mockford (2018) used WMO dust code analysis to suggest dust emissions occur year-round in Kangerlussuaq but that the highest frequency of dust event days is during spring (May, June) and autumn (September, October) and the lowest during July and August. During the spring 2017 sampling period, where the highest amount of dust deposition was recorded, only two dust codes were recorded at the airport weather station and these were both short-term (1 h) low intensity local events (code 6 and 7) (Table 3). By comparison, in spring 2018 one 'local' (code 7) and one 'severe' (code 34) dust event were recorded but dust deposition was < 10% of that recorded the previous spring. During the fall/winter 2018–2019 period five coded dust events were recorded, of which three were severe (code 34) and two local (codes 7 and 9) which was the highest frequency of code reporting during this study but corresponded to the lowest measured seasonal deposition rates. This suggests that for this 2-year period in Kangerlussuaq there is not a good relationship between dust proxy data and dust deposition rates, although the latter do suggest dust emissions can occur year-round and the highest deposition rate was recorded during the late spring/early summer which is line with Bullard and Mockford's (2018) conclusions from long-term dust code analysis. There are also inconsistencies between the dust code and visibility records. During spring 2017 visibility reduction of  $\leq 1$  km was recorded on 3 days which, if due to dust, suggests that three moderate dust storms (codes 30–32, 98) took place in addition to the two low intensity events that were recorded (Leys et al., 2011). Similarly, in spring 2018 visibility reduction to  $\leq 1$  km was recorded on nine different days but only two dust events were recorded.

Secondary dust records were examined here in an attempt to gain an insight into the magnitude and frequency of dust events that contributed to the overall dust deposition measured in each sampling period, however our analysis suggests that dust code and visibility data can not reliably be used in this way at this location. Bullard and Mockford (2018) suggest that topography in the Kangerlussuaq area may mean that small localized events, for example occurring up-valley on the Sandflugtsdalen outwash plain may not be recorded at the airport which is 16–20 km away. Similarly, dust events occurring near the airport as a result of deflation of the fjord delta sediments or anthropogenically-modified surfaces may be recorded as dust codes or reduced visibility but not contribute to dust deposition at the sites instrumented for this study located several kilometres away. Other recognized reasons for the lack of correspondence between dust code recording, visibility records and dust deposition include inconsistent and subjective classification of dust events (O'Loingsigh et al., 2010; Shao & Dong, 2006) and visibility reduction for reasons other than dust (e.g., fog, snow, rainfall, low cloud, smoke, haze) particularly in complicated high latitude atmospheric environments. The relationship between visibility and dust deposition may also be weakened if deposition is dominated by continuous low level background dust activity rather than episodic dust storm events (Cosentino et al., 2020).

### 4.3 | Regional patterns of dust deposition

The deposition of dust in periglacial environments contributes to the formation of loess deposits and loessic soils. Work on the source and distribution of such deposits has typically reported a decreasing depth of deposit comprising smaller particle sizes with distance from the sediment source that reflects the impact of atmospheric fallout and size-dependent settling of dust as it is transported downwind (Hugenholtz & Wolfe, 2010; Muhs et al., 2004; Schaetzl et al., 2021). Dijkmans and Törnqvist (1991) examined modern periglacial aeolian deposits around Kangerlussuaq and reported a slight decrease in grain size over a 6 km transect with increasing distance from the Sandflugstaldalen outwash plain. In their report, the proportion of material  $\leq 8 \mu\text{m}$  changed little over that distance and generally comprised  $< 5\%$  of the sediments, but the proportion of overall material  $\leq 63 \mu\text{m}$  increased from approximately 62% to 78%. Our results also indicate very little systematic change in the proportion of any size fraction with distance from the GrIS but do show a seasonal difference in the characteristics of dust deposits which has been reported elsewhere (Hugenholtz & Wolfe, 2010). In most seasons only a very small proportion of material deposited was coarser than  $90 \mu\text{m}$ , for example 0.24% in Spring 2017 (at SS1590) to 7.4% in Summer 2017 (at SS906), but in Summer 2018 at three sites  $> 15\%$  of captured material was  $\geq 90 \mu\text{m}$ . This may be due to localized reworking of loessic soils and high wind speeds at these sampling locations. In the Kangerlussuaq region, the lack of a clear regional gradient of decreasing particle-size or deposition rate likely reflects the distribution of multiple potential dust sources at different locations across the field areas, as well as the possibility of localized reworking or deflation of soils which can occur throughout the area (Heindel et al., 2015, 2017).

### 4.4 | Implications for interpretation of palaeoenvironmental records

The logistical constraints of measuring dust deposition at high latitudes over multiple seasons mean that terrestrial or lacustrine sediments are the primary means of determining long-term ( $> 10^1$ – $10^2$  years) dust deposition rates (e.g., Dorfman et al., 2015; Muhs et al., 2003; Müller et al., 2016; Sandgren & Fredskild, 1991). Although sedimentary records of minerogenic inputs can occasionally provide inter-annual records (e.g., Petterson et al., 2010) which allow direct comparisons between contemporary measured deposition rates and sediment-derived rates, they generally integrate over years and therefore reflect sub-decadal or longer trends (Viles & Goudie, 2003). In the Kangerlussuaq area, we have obtained two continuous years of modern dust deposition data. Previously in the same area long-term rates of dust deposition from sedimentary records have been determined (e.g., Saros et al., 2019). This provides an opportunity to compare historical (palaeo) with contemporary data.

Sedimentary records from low altitude peat profiles below the Ridge site suggest dust deposition rates varied from 75 to  $600 \text{ g m}^{-2} \text{ yr}^{-1}$  between 4750 cal. yr BP and modern times (Willemse et al., 2003). These high rates are likely to reflect the proximity of the sampling sites to the main dust source on the sandar. Holocene

records from two lakes close to the SS85 and SS1590 sites (c. 200 m altitude) used here have maximum minerogenic inputs around  $80 \text{ g m}^{-2} \text{ yr}^{-1}$  (Anderson et al., 2012). In all these records, highest minerogenic input occurs during the 200–300 years of the climatic deterioration of the Little Ice Age (LIA). Following the transition from the end of the Medieval Warm Period and onset of the LIA changes to the position of the GrIS margin may have led to an increase in jökulhlaup frequency (Storms et al., 2012) and the floodplain in Sandflugstaldalen underwent regeneration (Willemse et al., 2003). Both of these are likely to have increased sediment supply to the proglacial floodplain. Although wind velocities may have declined at the start of the LIA (Kuijpers & Mikkelsen, 2009), the onset of cold, dry conditions was ideal for subsequent deflation of the floodplain sediments because wind energy would have been more effective. As suggested by the contemporary data presented here (Figure 6) the increase in aeolian activity and deposition to lakes and other terrestrial sinks may have been the result of increased sediment supply and availability rather than an increase in wind speed. This supports the notion that dust deposition and particle-size characteristics can not necessarily be related to a single environmental driver but instead reflect the combined effects of multiple variables including sediment supply, availability, wind regime, precipitation, source location and, where present, vegetation (Újvári et al., 2016; Wang & Lai, 2014).

## 5 | CONCLUSIONS

Modern paraglacial environments have the potential to be important sources of contemporary dust and sinks for locally-derived dust deposition. Our measurements of dust deposition near the margin of the GrIS show that high latitude dust deposition occurs year-round. More dust was deposited during spring and summer than during the winter months. Our comparison of records of dust-related weather codes with field measurements of dust deposition for the Kangerlussuaq area show there is not a good relationship between dust proxy data and dust deposition rates over the short term. This may be due to the varied topography in this recently-deglaciated area but could also result from inconsistent or inaccurate recording of dust codes and visibility reduction.

Our measurements of annual dust deposition for each year are very different, but all remain consistent with the local to regional values expected from estimates for other locations at both high and low latitudes. For 2017–2018 and 2018–2019 the differences in annual dust deposition are accounted for by substantially higher dust deposition during a single season (spring 2017). Analysis of other local environmental data show this can be attributed to above average supply of sediment to the floodplain during 2016, which then became available for deflation during spring 2017, rather than an alternative driver such as strong winds. The importance of sediment supply, as compared to wind velocity, may have implications for the interpretation of palaeoenvironmental records as very high rates of aeolian deposition in sedimentary records may reflect sediment availability rather than an increase in wind speeds. Excluding spring 2017, there is a positive relationship between seasonal dust deposition and both air temperature and wind velocity. Any increase in air temperature in the Arctic may increase future aeolian deposition rates assuming sufficient sediment supply.

## ACKNOWLEDGEMENTS

This work was funded by a National Environmental Research Council award (NE/P011578/1) to JEB and NJA. MVS was funded by a Loughborough University PhD studentship. The authors thank Keechy Akkerman, Rebecca McKenzie, Tom Mockford, Suzanne McGowan and James Shilland for their help with field sampling and/or laboratory analyses. Chris Sorensen at the Kangerlussuaq International Sciences Support station provided invaluable logistical support. The data that support the findings of this study are available from the corresponding author upon reasonable request.

## DATA AVAILABILITY STATEMENT

The data that support the findings of this study are available from the corresponding author upon reasonable request.

## ORCID

Maud A. J. van Soest  <https://orcid.org/0000-0002-4656-515X>

Joanna E. Bullard  <https://orcid.org/0000-0002-2030-0188>

Clay Prater  <https://orcid.org/0000-0002-9864-6242>

Matthew C. Baddock  <https://orcid.org/0000-0003-1490-7511>

N. John Anderson  <https://orcid.org/0000-0002-0037-0306>

## REFERENCES

- Albani, S., Mahowald, N.M., Murphy, L.N., Raiswell, R., Moore, J.K., Anderson, R.F. et al. (2016) Paleodust variability since the Last Glacial Maximum and implications for iron inputs to the ocean. *Geophysical Research Letters*, 43, 3944–3954. Available from: <https://doi.org/10.1002/2016GL067911>
- Amino, T., Iizuka, Y., Matoba, S., Shimada, R., Oshima, N., Suzuki, T. et al. (2021) Increasing dust emission from ice free terrain in southeastern Greenland since 2000. *Polar Science*, 27, 100599. Available from: <https://doi.org/10.1016/j.polar.2020.100599>
- Anderson, N.J., Bullard, J.E., Cahoon, S.M.P., McGowan, S., Bagshaw, E.A., Barry, C.D. et al. (2017) The Arctic in the 21<sup>st</sup> century: changing biogeochemical linkages across a paraglacial landscape of Greenland. *Bioscience*, 67(2), 118–133. Available from: <https://doi.org/10.1093/biosci/biw158>
- Anderson, N.J., Harriman, R., Ryves, D.B. & Patrick, S.T. (2001) Dominant factors controlling variability in the ionic composition of west Greenland lakes. *Arctic, Antarctic, and Alpine Research*, 33(418), 425. Available from: <https://doi.org/10.1080/15230430.2001.12003450>
- Anderson, N.J., Liversidge, A.C., McGowan, S. & Jones, M.D. (2012) Lake and catchment response to Holocene environmental change: spatial variability along a climate gradient in southwest Greenland. *Journal of Paleolimnology*, 48(1), 209–222. Available from: <https://doi.org/10.1007/s10933-012-9616-3>
- Arnalds, O. (2010) Dust sources and deposition of aeolian materials in Iceland. *Icelandic Agricultural Sciences*, 23, 3–21.
- Arnalds, O., Olafsson, H. & Dagsson-Waldhauserova, P. (2014) Quantification of iron-rich volcanogenic dust emissions and deposition over the ocean from Icelandic dust sources. *Biogeosciences*, 11(23), 6623–6632. Available from: <https://doi.org/10.5194/bg-11-6623-2014>
- Baddock, M.C., Strong, C.L., Leys, J.F., Heindenreich, S.K., Tews, E.K. & McTainsh, G.H. (2014) A visibility and total suspended dust relationship. *Atmospheric Environment*, 89, 329–336. Available from: <https://doi.org/10.1016/j.atmosenv.2014.02.038>
- Beylich, A.A., Dickson, J.C. & Zwoliński, Z. (2016) *Source-to-sink Fluxes in Undisturbed Cold Environments*. Cambridge: Cambridge University Press, p. 419. [10.1017/CBO9781107705791](https://doi.org/10.1017/CBO9781107705791).
- Boy, M., Thomson, E.S., Acosta Navarro, J.C., Arnalds, O., Batchvarova, E., Back, J. et al. (2019) Interactions between the atmosphere, cryosphere and ecosystems at northern high latitudes. *Atmospheric Chemistry and Physics*, 19(3), 2015–2061. Available from: <https://doi.org/10.5194/acp-19-2015-2019>
- Bullard, J.E. (2013) Contemporary glacial inputs to the dust cycle. *Earth Surface Processes and Landforms*, 38(1), 71–89. Available from: <https://doi.org/10.1002/esp.3315>
- Bullard, J.E. (2017) The distribution and biogeochemical importance of high-latitude dust in the Arctic and Southern Ocean-Antarctic regions. *Journal of Geophysical Research-Atmospheres*, 122(5), 3098–3103. Available from: <https://doi.org/10.1002/2016JD026363>
- Bullard, J.E. & Austin, M.J. (2011) Dust generation on a proglacial floodplain, West Greenland. *Aeolian Research*, 3(1), 43–54. Available from: <https://doi.org/10.1016/j.aeolia.2011.01.002>
- Bullard, J.E., Baddock, M., Bradwell, T., Crusius, J., Darlington, E., Gaiero, D. et al. (2016) High-Latitude dust in the Earth system. *Reviews of Geophysics*, 54(2), 447–485. Available from: <https://doi.org/10.1002/2016RG000518>
- Bullard, J.E., Harrison, S.P., Baddock, M.C., Drake, N., Gill, T.E., McTainsh, G.H. et al. (2011) Preferential dust sources: a geomorphological classification designed for use in global dust models. *Journal of Geophysical Research*, 116(F4), F04034. Available from: <https://doi.org/10.1029/2011JF002061>
- Bullard, J.E. & McTainsh, G.H. (2003) Aeolian-fluvial interactions in dryland environments: examples, concepts and Australia case study. *Progress in Physical Geography*, 27(4), 471–501. Available from: <https://doi.org/10.1191/0309133303pp386ra>
- Bullard, J.E. & Mockford, T. (2018) Seasonal and decadal variability of dust observations in the Kangerlussuaq area, West Greenland. *Arctic, Antarctic, and Alpine Research*, 50(1), S100011. Available from: <https://doi.org/10.1080/15230430.2017.1415854>
- Bullard, J.E., Strong, S.L. & Aubault, H.A.P. (2022) Cyanobacterial soil crust responses to rainfall and effects on wind erosion in a semiarid environment, Australia: implications for landscape stability. *Journal of Geophysical Research: Biogeosciences*, 127(2), e2021JG006652. Available from: <https://doi.org/10.1029/2021JG006652>
- Comola, F., Giometto, M.G., Salesky, S.T., Parlange, M.B. & Lehning, M. (2019) Preferential deposition of snow and dust over hills: governing processes and relevant scales. *Journal of Geophysical Research-Atmospheres*, 124(14), 7951–7974. Available from: <https://doi.org/10.1029/2018JD029614>
- Cosentino, N.J., Gaiero, D.M. & Lambert, F. (2021) Present-Day Patagonian dust emissions: combining surface visibility, mass flux, and reanalysis data. *Journal of Geophysical Research-Atmospheres*, 126(16), e2020JD034459. Available from: <https://doi.org/10.1029/2020JD034459>
- Cosentino, N.J., Gaiero, D.M., Torea, G., Pasquini, A.I., Coppo, R., Arce, J.M. et al. (2020) Atmospheric dust dynamics in southern South America: a 14-year modern dust record in the loessic Pampean region. *The Holocene*, 30(4), 575–588. Available from: <https://doi.org/10.1177/0959683619875198>
- Crusius, J. (2021) Dissolved Fe supply to the Central Gulf of Alaska is inferred to be derived from Alaskan glacial dust that is not resolved by dust transport models. *Journal of Geophysical Research: Biogeosciences*, 126(6), e2021JG006323. Available from: <https://doi.org/10.1029/2021JG006323>
- Crusius, J., Schroth, A.W., Gassó, S., Moy, C.M., Levy, R.C. & Gatica, M. (2011) Glacial flour dust storms in the Gulf of Alaska: Hydrological and meteorological controls and their importance as a source of bioavailable iron. *Geophysical Research Letters*, 38(6), L06602. Available from: <https://doi.org/10.1029/2010GL046573>
- Dagsson-Waldhauserova, P., Arnalds, O. & Olafsson, H. (2013) Long-term frequency and characteristics of dust storm events in Northeast Iceland (1949–2011). *Atmospheric Environment*, 77, 117–127. Available from: <https://doi.org/10.1016/j.atmosenv.2013.04.075>
- Dagsson-Waldhauserova, P., Arnalds, O. & Olafsson, H. (2014) Long-term variability of dust events in Iceland (1949–2011). *Atmospheric Chemistry and Physics*, 14(24), 13411–13422. Available from: <https://doi.org/10.5194/acp-14-13411-2014>
- Dijkman, J.W.A. & Törnqvist, T.E. (1991) Modern periglacial eolian deposits and landforms in the Søndre Strømfjord area, West

- Greenland and their palaeoenvironmental implications. *Meddelelser om Grønland. Geoscience*, 25, 3–39.
- Dorfman, J.M., Stoner, J.S., Finkenbinder, M.S., Abbott, M.B., Xuan, C. & St-Onge, G. (2015) A 37,000-year environmental magnetic record of aeolian dust deposition from Burial Lake, Arctic Alaska. *Quaternary Science Reviews*, 128, 81–97. Available from: <https://doi.org/10.1016/j.quascirev.2015.08.018>
- Du, Z., Xiao, C., Dou, T., Li, S., An, H., Liu, S. et al. (2019) Comparison of Sr – Nd – Pb isotopes in insoluble dust between north-western China and high-latitude regions in the Northern Hemisphere. *Atmospheric Environment*, 214, 116837. Available from: <https://doi.org/10.1016/j.atmosenv.2019.116837>
- Eisner, W.R., Törnqvist, T.E., Koster, E.A., Bennike, O. & van Leeuwen, J.F.N. (1995) Paleocological studies of a Holocene lacustrine record from the Kangerlussuaq (Søndre Strømfjord) region of West Greenland. *Quaternary Research*, 43(1), 55–66. Available from: <https://doi.org/10.1006/qres.1995.1006>
- Engels, S. (2003) Modern and historical aeolian deposition rates in an uphill lake catchment in the Kangerlussuaq-region, West Greenland. *Internal Report, Faculty of Geographical Sciences*. Utrecht University
- Figgis, B., Guo, B., Javed, W., Ahzi, S. & Rémond, Y. (2018) Dominant environmental parameters for dust deposition and resuspension in desert climates. *Aerosol Science and Technology*, 52(7), 788–798. Available from: <https://doi.org/10.1080/02786826.2018.1462473>
- Fowler, R., Saros, J.E. & Osburn, C.L. (2018) Shifting DOC concentration and quality in the freshwater lakes of Kangerlussuaq region: an experimental assessment of possible mechanisms. *Arctic, Antarctic, and Alpine Research*, 50(1), S100013. Available from: <https://doi.org/10.1080/15230430.2018.1436815>
- Fristrup, B. (1953) Wind erosion within the Arctic Desserts. *Geografisk Tidsskrift*, 52, 51–65.
- Goossens, D. (1996) Wind tunnel experiments of aeolian dust deposition along ranges of hills. *Earth Surface Processes and Landforms*, 21(3), 205–216. Available from: [https://doi.org/10.1002/\(SICI\)1096-9837\(199603\)21:3<205::AID-ESP505>3.0.CO;2-T](https://doi.org/10.1002/(SICI)1096-9837(199603)21:3<205::AID-ESP505>3.0.CO;2-T)
- Goossens, D. (2006) Aeolian deposition of dust over hills: the effect of dust grain size on the deposition pattern. *Earth Surface Processes and Landforms*, 31(6), 762–776. Available from: <https://doi.org/10.1002/esp.1272>
- Groot Zwaafink, C.D., Grythe, H., Skov, H. & Stohl, A. (2016) Substantial contribution of northern high-latitude sources to mineral dust in the Arctic. *Journal of Geophysical Research-Atmospheres*, 121(13), 678–697. Available from: <https://doi.org/10.1002/2016JD025482>
- Hall, D.J., Upton, S.L. & Marsland, G.W. (1993) Designs for a deposition gauge and a flux gauge for monitoring ambient dust. *Atmospheric Environment*, 28(18), 2963–2979. Available from: [https://doi.org/10.1016/1352-2310\(94\)90343-3](https://doi.org/10.1016/1352-2310(94)90343-3)
- Hasholt, B., Mikkelsen, A.B., Nielsen, M.H. & Larsen, M.A.D. (2013) Observations of runoff and sediment and dissolved loads from the Greenland Ice Sheet at Kangerlussuaq, West Greenland, 2007–2010. *Zeitschrift für Geomorphologie*, 57(Supplementband 2), 3–27.
- Hasholt, B., van As, D., Mikkelsen, A.B., Mernild, S.H. & Yde, J.C. (2018) Observed sediment and solute transport from the Kangerlussuaq sector of the Greenland Ice Sheet (2006–2016). *Arctic Antarctic and Alpine Research*, 50(1), S100009. Available from: <https://doi.org/10.1080/15230430.2018.1433789>
- Heindel, R.C., Chipman, J.W. & Virginia, R.A. (2015) The spatial distribution and ecological impacts of aeolian soil erosion in Kangerlussuaq, West Greenland. *Annals of the Association of American Geographers*, 105(5), 875–890. Available from: <https://doi.org/10.1080/00045608.2015.1059176>
- Heindel, R.C., Culler, L.E. & Virginia, R.A. (2017) Rates and processes of aeolian soil erosion in West Greenland. *The Holocene*, 1–10(9), 1281–1290. Available from: <https://doi.org/10.1177/0959683616687381>
- Heindel, R.C., Governali, F.C., Spickard, A.M. & Virginia, R.A. (2019) The role of biological soil crusts in nitrogen cycling and soil stabilization in Kangerlussuaq, West Greenland. *Ecosystems*, 22(2), 243–256. Available from: <https://doi.org/10.1007/s10021-018-0267-8>
- Henkner, J., Scholter, T. & Kühn, P. (2016) Soil organic carbon stocks in permafrost-affected soils in West-Greenland. *Geoderma*, 282, 147–159. Available from: <https://doi.org/10.1016/j.geoderma.2016.06.021>
- Hobbs, W.H. (1931) Loess, Pebble Bands, and Boulders from Glacial Outwash of the Greenland Continental Glacier. *The Journal of Geology*, 39(4), 381–385. Available from: <https://doi.org/10.1086/623849>
- Hugenholtz, C.H. & Wolfe, S.A. (2010) Rates and environmental controls of aeolian dust accumulation, Athabasca River Valley, Canadian Rocky Mountains. *Geomorphology*, 121(3–4), 274–282. Available from: <https://doi.org/10.1016/j.geomorph.2010.04.024>
- Kidron, G.J., Zohar, M. & Starinsky, A. (2014) Spatial distribution of dust deposition within a small drainage basin: implications for loess deposits in the Negev Desert. *Sedimentology*, 61(7), 1908–1922. Available from: <https://doi.org/10.1111/sed.12121>
- Kocurek, G. (1998) Aeolian system response to external forcing factors – a sequence stratigraphic view of the Saharan region. In: Alsharhan, A.S., Glennie, K.W., Whittle, G.L. & Kendall, C.G.S.C. (Eds.) *Quaternary Deserts and Climatic Change*. Rotterdam, Netherlands: Balkema, pp. 327–349.
- Kuijpers, A. & Mikkelsen, N. (2009) Geological records of changes in wind regime over south Greenland since the Medieval Warm Period: a tentative reconstruction. *Polar Record*, 45(1), 1–8. Available from: <https://doi.org/10.1017/S0032247408007699>
- Lancaster, N. (2002) Flux of eolian sediment in the McMurdo Dry Valleys, Antarctica: a preliminary assessment. *Arctic Antarctic and Alpine Research*, 3(3), 318–323. Available from: <https://doi.org/10.2307/1552490>
- Lawrence, C.R. & Neff, J.C. (2009) The contemporary physical and chemical flux of aeolian dust: A synthesis of direct measurements of dust deposition. *Chemical Geology*, 267(1–2), 46–63. Available from: <https://doi.org/10.1016/j.chemgeo.2009.02.005>
- Leys, J.F., Heidenreich, S.K., Strong, C.L., McTainsh, G.H. & Quigley, S. (2011) PM10 concentrations and mass transport during “Red Dawn” – Sydney 23 September 2009. *Aeolian Research*, 3(3), 327–342. Available from: <https://doi.org/10.1016/j.aeolia.2011.06.003>
- Li, J., Garshick, E., Huang, S. & Kourakis, P. (2021) Impacts of El Niño–Southern Oscillation on surface dust levels across the world during 1982–2019. *Science of the Total Environment*, 769, 144566. Available from: <https://doi.org/10.1016/j.scitotenv.2020.144566>
- Lund-Hansen, L.C., Andersen, T.J., Nielsen, M.H. & Pejrup, M. (2010) Suspended matter, Chl-a, CDOM, grain sizes and optical properties in the Arctic fjord-type estuary, Kangerlussuaq, West Greenland, during summer. *Estuaries and Coasts*, 33(6), 1442–1451. Available from: <https://doi.org/10.1007/s12237-010-9300-7>
- Mahowald, N.M., Ballantine, J.A., Feddema, J. & Ramankutty, N. (2007) Global trends in visibility: implications for dust sources. *Atmospheric Chemistry and Physics*, 7(12), 3309–3339. Available from: <https://doi.org/10.5194/acp-7-3309-2007>
- Mao, R., Ho, C.H., Feng, S., Gong, D.Y. & Shao, Y.P. (2013) The influence of vegetation variation on Northeast Asian dust activity. *Asia-Pacific Journal of Atmospheric Sciences*, 49(1), 87–94. Available from: <https://doi.org/10.1007/s13143-013-0010-5>
- Marx, S.K. & McGowan, H.A. (2005) Dust transportation and deposition in a superhumid environment, West coast, South Island, New Zealand. *Catena*, 59(2), 147–171. Available from: <https://doi.org/10.1016/j.catena.2004.06.005>
- Marx, S.K., McGowan, H.A. & Kamber, B.S. (2009) Long-range dust transport from eastern Australia: a proxy for Holocene aridity and ENSO-type climate variability. *Earth and Planetary Science Letters*, 282(1–4), 167–177. Available from: <https://doi.org/10.1016/j.epsl.2009.03.013>
- McTainsh, G.H., Leys, J.F. & Nickling, W.G. (1998) Wind erodibility of arid lands in the Channel Country of western Queensland, Australia. *Zeitschrift für Geomorphologie, Supplementbände*, 116, 113–130.
- Mockford, T., Bullard, J.E. & Thorsteinsson, T. (2018) The dynamic effects of sediment availability on the relationship between wind speed and dust concentration. *Earth Surface Processes and Landforms*, 43(11), 2484–2492. Available from: <https://doi.org/10.1002/esp.4407>

- Muhs, D.R. (2013) The geologic record of dust in the Quaternary. *Aeolian Research*, 9, 3–48. Available from: <https://doi.org/10.1016/j.aeolia.2012.08.001>
- Muhs, D.R., Ager, T.A., Been, J., Bradbury, J.P. & Dean, W.E. (2003) A late Quaternary record of eolian silt deposition in a maar lake, St. Michael Island, western Alaska. *Quaternary Research*, 60(1), 110–122. Available from: [https://doi.org/10.1016/S0033-5894\(03\)00062-0](https://doi.org/10.1016/S0033-5894(03)00062-0)
- Muhs, D.R., McGeehin, J.P., Beann, J. & Fisher, E. (2004) Holocene loess deposition and soil formation as competing processes, Matanuska Valley, southern Alaska. *Quaternary Research*, 61(3), 265–276. Available from: <https://doi.org/10.1016/j.yqres.2004.02.003>
- Müller, M., Thiel, C. & Kühn, P. (2016) Holocene palaeosols and aeolian activities in the Umimallissuaq valley, West Greenland. *The Holocene*, 26(7), 1149–1161. Available from: <https://doi.org/10.1177/0959683616632885>
- Nakashima, M. & Dagsson-Waldhauserová, P. (2019) A 60 year examination of dust day activity and its contributing factors from ten Icelandic weather stations from 1950 to 2009. *Frontiers in Earth Science*, 6, 245. Available from: <https://doi.org/10.3389/feart.2018.00245>
- Oerlemans, J., Giesen, R.H. & Van den Broeke, M.R. (2009) Retreating alpine glaciers: increased melt rates due to accumulation of dust (Vadret da Morteratsch, Switzerland). *Journal of Glaciology*, 55(192), 729–736. Available from: <https://doi.org/10.3189/002214309789470969>
- Offer, Z.Y. & Goossens, D. (2004) Thirteen years of aeolian dust dynamics in a desert region (Negev desert, Israel): analysis of horizontal and vertical dust flux, vertical dust distribution and dust grain size. *Journal of Arid Environments*, 57(1), 117–140. Available from: [https://doi.org/10.1016/S0140-1963\(03\)00092-2](https://doi.org/10.1016/S0140-1963(03)00092-2)
- O'Hara, S., Clarke, M.L. & Elatrach, M.S. (2006) Field measurements of desert dust deposition in Libya. *Atmospheric Environment*, 40(21), 3881–3897. Available from: <https://doi.org/10.1016/j.atmosenv.2006.02.020>
- O'Loingsigh, T., McTainsh, G.H., Tapper, N.J. & Shinkfield, P. (2010) Lost in code: a critical analysis of using meteorological data for wind erosion monitoring. *Aeolian Research*, 2(1), 49–57. Available from: <https://doi.org/10.1016/j.aeolia.2010.03.002>
- O'Loingsigh, T., McTainsh, G.H., Tews, E.K., Strong, C.L., Leys, J.F., Shinkfield, P. et al. (2014) The Dust Storm Index (DSI): a method for monitoring broadscale wind erosion using meteorological records. *Aeolian Research*, 12, 29–40. Available from: <https://doi.org/10.1016/j.aeolia.2013.10.004>
- Owens, P.N. & Slaymaker, O. (1997) Contemporary and post-glacial rates of aeolian deposition in the coast mountains of British Columbia, Canada. *Geografiska Annaler, Series a*, 79(4), 267–276. Available from: <https://doi.org/10.1111/j.0435-3676.1997.00022.x>
- Ozols, U. & Broll, G. (2003) Soil Ecological processes in vegetation patches of well drained permafrost affected sites (Kangerlussuaq - West Greenland). *Polarforschung*, 73, 5–14.
- Petterson, G., Renberg, I., Sjøstedt-de Luna, S., Arnqvist, P. & Anderson, N.J. (2010) Climatic influence on the inter-annual variability of late-Holocene minerogenic sediment supply in a boreal forest catchment. *Earth Surface Processes and Landforms*, 35, 390–398. Available from: <https://doi.org/10.1002/esp.1933>
- Prater, C., Bullard, J.E., Osburn, C.L., Martin, S.L., Watts, M.J. & Anderson, N.J. (2021) Landscape controls on nutrient stoichiometry regulate lake primary production at the margin of the Greenland Ice Sheet. *Ecosystems*. Available from: <https://doi.org/10.1007/s10021-021-00693-x>
- Prospero, J.M., Bullard, J.E. & Hodgkins, R. (2012) High-latitude dust over the North Atlantic: inputs from Icelandic proglacial dust storms. *Science*, 335(6072), 1078–1082. Available from: <https://doi.org/10.1126/science.1217447>
- Reheis, M.C. & Urban, F.E. (2011) Regional and climatic controls on seasonal dust deposition in the southwestern US. *Aeolian Research*, 3(1), 3–21. Available from: <https://doi.org/10.1016/j.aeolia.2011.03.008>
- Rydberg, J., Lindborg, T., Sohlenius, G., Reuss, N., Olsen, J. & Laudon, H. (2016) The importance of eolian input on lake-sediment geochemical composition in the dry proglacial landscape of West Greenland. *Arctic Antarctic and Alpine Research*, 48(1), 93–109. Available from: <https://doi.org/10.1657/AAAR0015-009>
- Rymer, K.G., Rachlewicz, G., Buchwal, A., Temme, A.J.A.M., Reimann, T. & van der Meij, W.M. (2022) Contemporary and past aeolian deposition rates in periglacial conditions (Ebba Valley, central Spitsbergen). *Catena*, 211, 105974. Available from: <https://doi.org/10.1016/j.catena.2021.105974>
- Sandgren, P. & Fredskild, B. (1991) Magnetic measurements recording Late Holocene man-induced erosion in S. Greenland. *Boreas*, 20(4), 315–331. Available from: <https://doi.org/10.1111/j.1502-3885.1991.tb00283.x>
- Saros, J.E., Anderson, N.J., Juggins, S., McGowan, S., Yde, J.C., Telling, J. et al. (2019) Arctic climate shifts drive rapid ecosystem responses across the West Greenland landscape. *Environmental Research Letters*, 14(7), 074027. Available from: <https://doi.org/10.1088/1748-9326/ab2928>
- Schaetzl, R.J., Nyland, K.E., Kasmerchak, C.S., Breeze, V., Kamoske, A., Thomas, S.E. et al. (2021) Holocene silty-sand loess downwind of dunes in Northern Michigan, USA. *Physical Geography*, 42(1), 25–49. Available from: <https://doi.org/10.1080/02723646.2020.1734414>
- Schmale, J., Zieger, P. & Ekman, A.M.L. (2021) Aerosols in current and future Arctic climate. *Nature Climate Change*, 11(2), 95–105. Available from: <https://doi.org/10.1038/s41558-020-00969-5>
- Shao, Y. & Dong, C.H. (2006) A review on East Asian dust storm climate, modelling and monitoring. *Global and Planetary Change*, 52(1-4), 1–22. Available from: <https://doi.org/10.1016/j.gloplacha.2006.02.011>
- Sow, M., Goossens, D. & Rajot, J.L. (2006) Calibration of the MDCO dust collector and of four versions of the inverted frisbee dust deposition sampler. *Geomorphology*, 82(3-4), 360–375. Available from: <https://doi.org/10.1016/j.geomorph.2006.05.013>
- Storms, J.E.A., de Winter, I.L., Overeem, I., Drijkoningen, G.G. & Lykke-Andersen, H. (2012) The Holocene sedimentary history of the Kangerlussuaq Fjord-valley fill, West Greenland. *Quaternary Science Reviews*, 35, 29–50. Available from: <https://doi.org/10.1016/j.quascirev.2011.12.014>
- Tedesco, M., Box, J.E., Cappelen, J., Fausto, R.S., Fettweis, X., Andersen, J.K. et al. (2018) *Greenland Ice Sheet* [in Arctic Report Card 2018], <https://www.arctic.noaa.gov/Report-Card>
- Tegen, I. (2003) Modeling the mineral dust aerosol cycle in the climate system. *Quaternary Science Reviews*, 22(18-19), 1821–1834. Available from: [https://doi.org/10.1016/S0277-3791\(03\)00163-X](https://doi.org/10.1016/S0277-3791(03)00163-X)
- Tobo, Y., Adachi, K., DeMott, P.J., Hill, T.C.J., Hamioton, D.S., Mahowald, N.M. et al. (2019) Glacially sourced dust as a potentially significant source of ice nucleating particles. *Nature Geoscience*, 12(4), 253–258. Available from: <https://doi.org/10.1038/s41561-019-0314-x>
- Tsoar, H. & Pye, K. (1987) Dust transport and the question of desert loess formation. *Sedimentology*, 34(1), 139–153. Available from: <https://doi.org/10.1111/j.1365-3091.1987.tb00566.x>
- Újvári, G., Kok, J.F., Varga, G. & Kovács, J. (2016) The physics of wind-blown loess: implications for grain size proxy interpretations in Quaternary paleoclimate studies. *Earth-Science Reviews*, 154, 247–278. Available from: <https://doi.org/10.1016/j.earscirev.2016.01.006>
- van As, D., Hasholt, B., Ahlstrøm, A.P., Box, J.E., Cappelen, J., Colgan, W. et al. (2019). Programme for monitoring of the Greenland ice sheet (PROMICE): Watson River discharge. Version: v01, Dataset published via Geological Survey of Denmark and Greenland. [https://doi.org/10.22008/promice/data/watson\\_river\\_discharge](https://doi.org/10.22008/promice/data/watson_river_discharge)
- vanCuren, R.A., Cahill, T., Burkhart, J., Barnes, D., Zhao, Y., Perry, K. et al. (2012) Aerosols and their sources at Summit Greenland – first results of continuous size- and time-resolved sampling. *Atmospheric Environment*, 52, 82–97. Available from: <https://doi.org/10.1016/j.atmosenv.2011.10.047>
- Varga, G., Dagsson-Waldhauserová, P., Gresina, F. & Helgadottir, A. (2021) Saharan dust and giant quartz particle transport towards Iceland. *Scientific Reports*, 11(1), 11891. Available from: <https://doi.org/10.1038/s41598-021-91481-z>
- Viles, H.A. & Goudie, A.S. (2003) Interannual, decadal and multidecadal scale climatic variability and geomorphology. *Earth-Science Reviews*,

- 61(1–2), 105–131. Available from: [https://doi.org/10.1016/S0012-8252\(02\)00113-7](https://doi.org/10.1016/S0012-8252(02)00113-7)
- Wang, Y.Q., Zhang, X.Y., Gong, S.L., Zhou, C.H., Hu, X.Q., Liu, H.L. et al. (2008) Surface observation of sand and dust storm in East Asia and its application in CUACE/Dust. *Atmospheric Chemistry and Physics*, 8(3), 545–553. Available from: <https://doi.org/10.5194/acp-8-545-2008>
- Wang, Z.-T. & Lai, Z.-P. (2014) A theoretical model on the relation between wind speed and grain size in dust transportation and its palaeoclimatic implications. *Aeolian Research*, 13, 105–108. Available from: <https://doi.org/10.1016/j.aeolia.2014.04.003>
- Willemsse, N.W., Koster, E.A., Hoogakker, B. & van Tatenhove, F.G.M. (2003) A continuous record of Holocene eolian activity in West Greenland. *Quaternary Research*, 59(3), 322–334. Available from: [https://doi.org/10.1016/S0033-5894\(03\)00037-1](https://doi.org/10.1016/S0033-5894(03)00037-1)
- Xi, X. (2021) Revisiting the recent dust trends and climate drivers using horizontal visibility and present weather observations. *Journal of Geography Research: Atmospheres*, 126, e2020JD034687. Available from: <https://doi.org/10.1029/2021JD034687>
- Yde, J.C., Anderson, N.J., Post, E., Saros, J.E. & Telling, J. (2018) Environmental change and impacts in the Kangerlussuaq area, West Greenland. *Arctic, Antarctic, and Alpine Research*, 50(1), S100001. Available from: <https://doi.org/10.1080/15230430.2018.1433786>
- Zender, C.S. & Kwon, E.Y. (2005) Regional contrasts in dust emission responses to climate. *Journal of Geophysical Research-Atmospheres*, 110, D13201. Available from: <https://doi.org/10.1029/2004JD005501>

**How to cite this article:** van Soest, M.A.J., Bullard, J.E., Prater, C., Baddock, M.C. & Anderson, N.J. (2022) Annual and seasonal variability in high latitude dust deposition, West Greenland. *Earth Surface Processes and Landforms*, 47(10), 2393–2409. Available from: <https://doi.org/10.1002/esp.5384>